Reducing cambers and prestress losses by including fully tensioned top prestressing strands and mild reinforcing steel

Hema Jayaseelan and Bruce W. Russell

- The inclusion of fully tensioned top strands and mild reinforcing steel in the precompression zones of prestressed concrete bridge girders can reduce total camber by as much as 72%.
- This paper compares four existing methods for estimating prestress losses in prestressed concrete bridge girders and presents a new method for estimating prestress losses
- Prestress losses were calculated with each method to compare the results from the different methods, which were then used to determine the effects of adding fully tensioned top strands and mild reinforcing steel to the cross section.

PCI Journal (ISSN 0887-9672) V. 64, No. 3, May–June 2019.
PCI Journal is published bimonthly by the Precast/Prestressed Concrete Institute, 200 W. Adams St., Suite 2100, Chicago, IL 60606.

Nearly two-thirds of new highway bridges in the United States are constructed using precast, prestressed concrete girders. In the past two decades, the widespread use of high-performance concrete (HPC) has permitted longer spans, larger girder spacings, and shallower depths for prestressed concrete bridges.[1] HPC has a lower water–cementitious material ratio than traditional concrete. Coupled with the inclusion of supplementary cementitious materials, HPC offers dramatic improvements in concrete quality and durability. The use of HPC produces precast, prestressed concrete bridges that are both economical and possess long life expectancies, which is vital to building and maintaining a sustainable transportation infrastructure.

The primary objective of this research is to examine the effects that fully tensioned top strands and the inclusion of mild reinforcing steel have on prestress losses and camber of pretensioned bridge girders. The paper also presents various methods of computing prestress losses, including older PCI methods and methods found in the 2014 American Association of State Highway and Transportation Officials' *AASHTO LRFD Bridge Design Specifications*.[2] This paper investigates the effectiveness of including mild reinforcing steel and fully tensioned top strands as techniques to reduce prestress losses and cambers, develops a time-step method that accounts for recent changes to the AASHTO LRFD specifications, and compares the results of the various methods. The results demonstrate that the inclusion of both fully tensioned top strands and mild reinforcing steel reduces both prestress losses and cambers. The reductions in prestress

losses are small. The top strand reduced losses by only 8% and mild reinforcing steel reduced losses by only 5% for the cases examined, but the reductions in predicted cambers for bridge girders are significant (as large as 45% and 24% for the inclusion of fully tensioned top strands and mild reinforcing steel, respectively), with about a 72% reduction in camber with the combination of both fully tensioned top strands and mild reinforcing steel. The paper demonstrates that these two techniques, when put to use, will translate into improvements in long-term bridge performance and ride quality.

Background

Efficient design of prestressed concrete bridges requires accurate prediction of prestress losses and cambers. The four primary sources of prestress losses in pretensioned bridge girders are elastic shortening, concrete creep, concrete shrinkage, and steel relaxation. Seating losses also occur prior to detensioning strands but are usually not as significant for pretensioned bridge girders as the other losses. This paper shows that prestress losses are affected by structural detailing, such as the number and size of prestressing strands, the eccentricity of the prestressing force, girder spacing, and girder spans. In addition, prestress losses are affected by variations in the material properties of the concrete. The elastic modulus, creep coefficient, and shrinkage characteristics of the concrete are all affected by the concrete mixture proportions and by the overall quality of the aggregates and their shapes and sizes. The variables in concrete material properties are largely unaccounted for in traditional computations for prestress losses, particularly when the contract and construction processes separate design functions from fabrication and construction.

Numerous research programs have been conducted, and a variety of prestress loss prediction methods have been proposed;[3,4] however, the accurate determination of prestress losses has always been a challenge. Inaccurate predictions of prestress losses often result in large cambers of prestressed concrete bridge girders and in differential cambers in girders of identical design for the same spans on the same bridge. Excessive camber can, in turn, adversely affect the bridge's serviceability. Poor prediction of prestress losses can also lead to increasing the number of prestressing strands, which can lead to greater cambers and increased cracking in girder end regions, adversely affecting the durability, ride quality, and overall performance of the bridge.

In the late 1950s and early 1960s, the American Concrete Institute–American Society of Civil Engineers (ACI-ASCE) Joint Committee 423[5] proposed a lump-sum method for estimating prestress losses. These losses included the effects of elastic shortening, creep, shrinkage, and relaxation but excluded frictional and anchorage losses. The further refinement of prestress loss calculation methods led to the development of recommendations by the PCI Prestress Losses Committee,[6] the AASHTO *Standard Specifications for Highway Bridges* method,[7] and the ACI-ASCE Committee recommendations directed by Paul Zia and reported in *Concrete International*.[8] However, these methods for calculating prestress losses failed to account for the variability of the concrete material properties, which led to overestimation or underestimation of losses.[3,9–11]

The National Cooperative Highway Research Program (NCHRP) investigated the measurement of concrete material properties and cross-section properties that effect measured prestress losses and deflections.[3] These include elastic modulus, concrete strength, volume–to–surface area ratio *V*/*S*, and creep coefficient. New equations for prestress losses were proposed. The experimental research conducted on prestressed concrete bridge girders by Tadros et al.,[3] Gruel et al.,[10] Pessiki et al.,[12] and Hale and Russell[11] verified that the *PCI Design Handbook*[8] method and the 1998 AASHTO LRFD specifications[13] equations overestimated the prestress losses. The issues related to camber and deflection were not discussed in detail, but it was concluded that accurate determination of losses was necessary for the more precise prediction of camber or deflection.

Figure 1. North Canadian River overflow structure, John Kilpatrick Turnpike, Okla., consisting of nineteen 103 ft 4 in. (31.5 m) spans in both northbound and southbound directions with Type IV girders spaced at 8 ft 9 in. (2.7 m) on center.

Figure 2. View underneath the North Canadian River overflow structure, John Kilpatrick Turnpike, Okla.

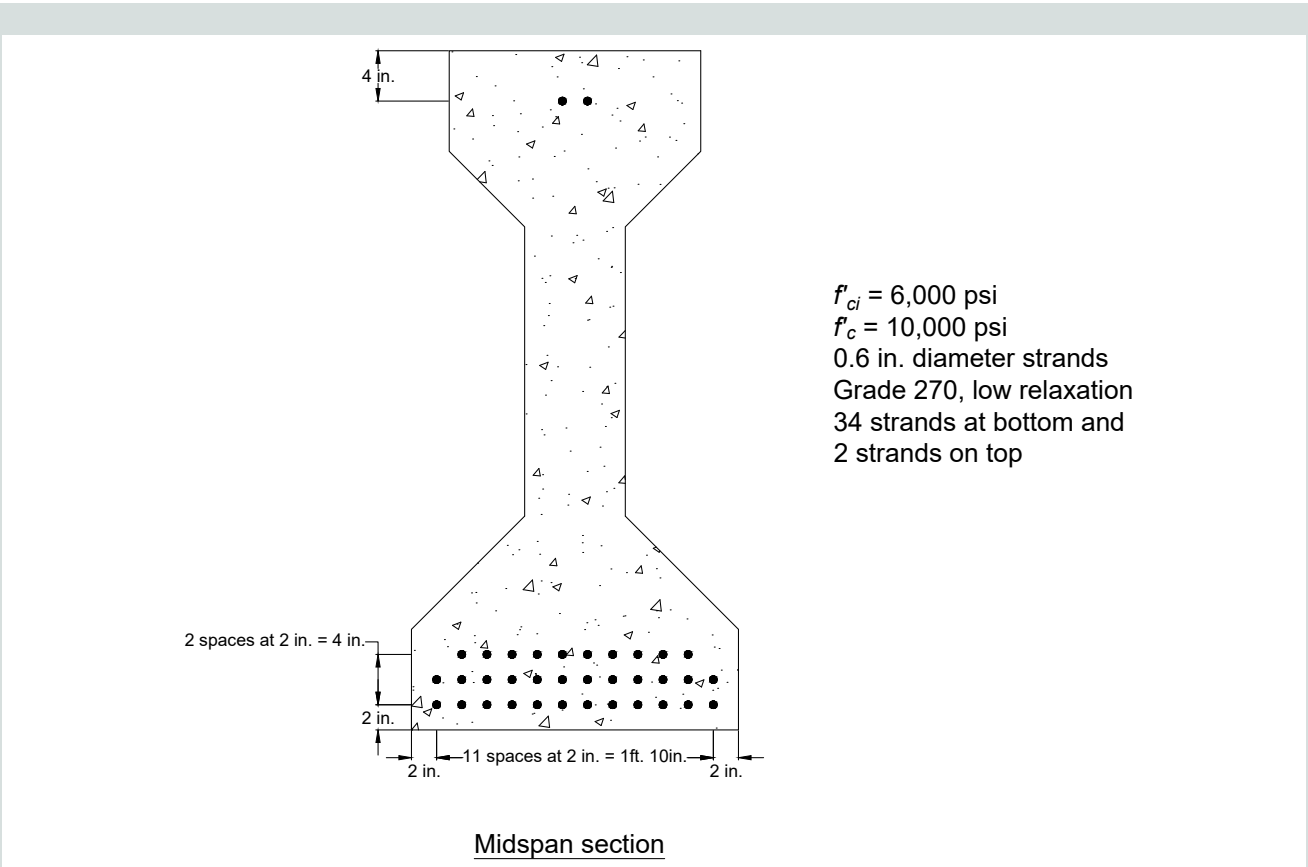

Figure 3. Type IV cross section with thirty-four 0.6 in. (15 mm) diameter strands in the bottom flange. Note: f'_c = specified concrete compressive strength; f'_{ci} = specified concrete compressive strength at release. 1 in. = 25.4 mm; 1 ft = 0.305 m; 1 psi = 6.895 kPa; Grade 270 = 1860 MPa.

Methodology

The analyses in this paper are based on the North Canadian River overflow structure, which was built around 2000 on the John Kilpatrick Turnpike in Oklahoma. This bridge features 19 spans in both the northbound and southbound directions, with Type IV girders spanning 103 ft 4 in. (31.5 m) from center to center of bearing. The cast-in-place concrete deck slab is 8 in. (200 mm) thick and has a specified concrete compressive strength f'_c of 5000 psi (34.5 MPa). Both the northbound and southbound structures are 41 ft (12.5 m) wide, with five girders spaced at 8 ft 9 in. (2.7 m). Only the interior girder design was considered for this paper.

Figures 1 and **2** show the overflow structure. **Figure 3** shows the cross section of the Type IV girder with the strand pattern at midspan. Two top strands are shown for illustration, but the number of top strands was a variable (none, two, or four) in this research. The original design and actual construction of the girders included six draped strands. For the purposes of our research, the strand patterns were converted to straight strand patterns following current practice in Oklahoma. Debonding was provided at end regions to control compressive stresses at release.

In the analyses performed for this paper, prestress losses were computed at both the girder end regions and at midspan. The following methods were used to compute or estimate prestress losses:

- the *PCI Design Handbook* method, based on Zia et al.[8]
- a modified version of the *PCI Design Handbook* method using transformed cross-section properties in lieu of gross-section properties
- the 2014 AASHTO LRFD specifications,[2] approximate estimates of total losses
- the 2014 AASHTO LRFD specifications, refined estimates of time-dependent losses
- the Jayaseelan time-step method, developed by the authors, adopting time-dependent formulations from ACI 209,[14] the 2014 AASHTO LRFD specifications, and other relevant sources[15,16]

The primary purpose of this paper is to investigate variations in prestress losses and in bridge girder camber that result from the following variables:

- differences in methodology

- inclusion of fully tensioned top strands (none, two, or four strands)
- inclusion of nonprestressed mild reinforcing steel (none, 2.4 in.^{2}, or 5.0 in.^{2} [none, 1550 mm^2, or 3230 mm^2]) at the center of gravity of the prestressing strands

Methods and results

The prestress losses were calculated with each method for five different girder design cases:

- a base case, which represents the design without top strands and without mild reinforcing steel
- T2 and T4, for which there are either two or four fully tensioned top strands, respectively
- MS 2.4, which includes four no. 7 (22M) mild reinforcing bars at the center of gravity of the prestressing strands
- and MS 5.0, which includes five no. 9 (29M) mild reinforcing bars at the center of gravity of the prestressing strands

The prestress losses were computed using a spreadsheet algorithm for all cases and all methods.

PCI Design Handbook method

At the time of its publication, the *PCI Design Handbook*[8] method offered the descriptive method to quantify factors that influence prestress losses. Even though more detailed methods of estimating losses have since been developed, the original method remains a valuable tool for estimating prestress losses for all types of precast, prestressed concrete structural members. Although this simple method is now used primarily for building products, the principles it sets forth are time tested and remain valid.

In our analysis, gross-section properties were used as described in Zia et al.[8] All of the concrete stress parameters taken at the center of gravity of the strands, such as stress due to the prestressing force f_{cpi}, net compressive stress immediately after the prestress has been applied f_{cir}, stress due to the weight of the structure at the time prestress is applied f_g, and stress due to superimposed permanent dead loads f_{cds}, were computed as described in Zia et al.[8] The adjustment factor for elastic shortening K_{es} was taken as 1.0 for pretensioned concrete, and the stress adjustment factor for elastic shortening and steel relaxation K_{cir} was taken as 0.90, without alteration or iteration. The adjustment factor for creep K_{cr} was 2.0, and the adjustment factor for shrinkage K_{sh} was 1.0 for pretensioned members. The prestressing force in tendons P_{pi} after seating loss but before reduction for elastic shortening (*ES*), creep (*CR*), shrinkage (*SH*), and relaxation (*RE*) was computed as follows:

$$P_{pi} = A_{ps} \times 0.75 f_{pu}$$

where

A_{ps} = area of prestressing strands

f_{pu} = ultimate strength of prestressing strand

Seating losses occurred at tensioning before other losses occurred. The modulus of elasticity of the prestressing strand E_{ps} was taken as 28,500 ksi (196.5 GPa), and the initial or design modulus of elasticity of concrete, E_{ci} or E_c, respectively, was estimated using the equation given in *Building Code Requirements for Structural Concrete (ACI 318-14) and Commentary (ACI 318R-14)* section 19.2.2.1.a:[17]

$$E_c = 33w^{1.5}(f'_c)^{0.5} \qquad \text{(ACI 318-14 19.2.2.1.a)}$$

where

w = unit weight of concrete in lb/ft^3

Table 1 shows the computed prestress losses from the *PCI Design Handbook* method. Note that this method can account for the effects of top strands as the initial prestressing force P_{pi} and its eccentricity e change with changes in strand patterns. Alternatively, the method does not have a way to account for the effects of mild reinforcing steel. Prestress loss due to shrinkage *SH* is the same for all cases because it depends on the assumed ultimate shrinkage strain (550×10^{-6} in./in. [550×10^{-6} mm/mm]), the relative humidity *RH* (65% for central Oklahoma), and the volume–to–surface area ratio *V*/*S*, which do not change from case to case. Prestress loss due to creep *CR* is computed using the same method for either 90 days or 10,000 days, and different values for *CR* are reported for the two concrete ages. But this method does not truly account for the effects of time; instead, the difference in value comes from the difference in concrete stress resulting from sustained dead load f_{cds}. At 90 days the slab's dead load is not included in f_{cds}, and at 10,000 days the dead load from the slab is included. The base case (no top strands and no mild reinforcing steel) shows total prestress losses *TL* of 53.5 ksi (369 MPa) at 90 days, and the inclusion of top strands (T4) reduces this to 48.5 ksi (334 MPa). Using the *PCI Design Handbook* method, the inclusion of top strands reduces *TL* from 53.5 to 48.5 ksi at 90 days.

PCI Design Handbook method using transformed cross-section properties

The *PCI Design Handbook* method is repeated; however, the prestress losses were computed using transformed cross-section properties. Cross-section properties and other parameters are computed using the same formulas but using transformed cross-section properties in place of gross-section properties. In this analysis, all of the stress parameters for the *PCI Design Handbook* method were computed using transformed cross sections. One of the differences when using transformed section properties is that a value for f_{cpi} is not needed to compute the loss due to elastic shortening *ES*; instead, f_{cir} is

Table 1. Prestress losses at midspan calculated using gross-section properties with the *PCI Design Handbook* method

Case	Concrete age, days	*ES*, ksi	*CR*, ksi	*SH*, ksi	*RE*, ksi	Losses at midspan, ksi
Base	90	17.5	27.2	5.8	3.0	53.5
	10,000	17.5	13.3	5.8	3.5	40.1
T2	90	16.3	25.3	5.8	3.1	50.5
	10,000	16.3	13.0	5.8	3.6	38.7
T4	90	15.5	24.0	5.8	3.2	48.5
	10,000	15.5	13.2	5.8	3.6	38.1
MS 2.4	90	Prestress losses same as base case				
	10,000					
MS 5.0	90					
	10,000					

Note: *CR* = prestress loss due to creep; *ES* = prestress loss due to elastic shortening; *RE* = prestress loss due to relaxation; *SH* = prestress loss due to shrinkage. 1 ksi = 6.895 MPa.

computed directly using transformed cross-section properties, with K_{cir} taken as 1.0. *ES* becomes a more direct computation once the transformed cross-section properties are computed. Note that when using transformed cross-section properties, the inclusion of mild reinforcing steel affects the computation of losses and the effects of mild reinforcing steel can be taken into account.

As in the original *PCI Design Handbook* method (using gross-section properties), *SH* is the same for all cases because the inclusion of additional reinforcement affects neither *RH* nor *V*/*S*. Minor changes in *CR* are caused by inclusion of the top strands and mild reinforcing steel. The small changes in *CR* reflect the effects of the top strands on prestressed eccentricity and its inclusion in the transformed cross-section properties. **Table 2** reports the prestress losses computed using this method.

AASHTO LRFD specifications approximate estimates of time-dependent prestress losses

Computation of prestress losses for this analysis follows the methods and procedures given in the 2014 AASHTO LRFD specifications.[2] Estimates of long-term prestress losses resulting from creep and shrinkage of concrete and from relaxation of prestressing strands (*CR* + *SH* + *RE*) were calculated using AASHTO LRFD specifications Eq. 5.9.5.3-1b. *ES* is comput-

Table 2. Prestress losses at midspan calculated using transformed cross-section properties with the *PCI Design Handbook* method

Case	Concrete age, days	*ES*, ksi	*CR*, ksi	*SH*, ksi	*RE*, ksi	Losses at midspan, ksi
Base	90	18.2	28.2	5.8	2.9	55.1
	10,000	18.2	15.6	5.8	3.4	43.0
T2	90	17.0	26.4	5.8	3.0	52.2
	10,000	17.0	15.2	5.8	3.5	41.5
T4	90	16.3	25.2	5.8	3.1	50.3
	10,000	16.3	15.3	5.8	3.5	40.8
MS 2.4	90	17.6	27.2	5.8	3.0	53.5
	10,000	17.6	15.1	5.8	3.5	41.9
MS 5.0	90	17.0	26.3	5.8	3.0	52.1
	10,000	17.0	14.6	5.8	3.5	40.8

Note: *CR* = prestress loss due to creep; *ES* = prestress loss due to elastic shortening; *RE* = prestress loss due to relaxation; *SH* = prestress loss due to shrinkage. 1 ksi = 6.895 MPa.

ed independently in the prescribed method (which closely resembles other methods). The total prestress losses *TL* are obtained by adding *ES* to the estimate for time-dependent losses (*CR* + *SH* + *RE*). **Table 3** gives the results for prestress losses computed with this method. The equations do not account for the inclusion of mild reinforcing steel. The addition of fully tensioned top strands affects *ES* and changes the parameters in the equation for long-term losses, so changes due to fully tensioned top strands are reflected in Table 3, even though the changes are relatively small.

AASHTO LRFD specifications refined estimates of time-dependent prestress losses

Computation of prestress losses for this analysis follows the methods and procedures given in the 2014 AASHTO LRFD specifications, article (5.9.5.4.1).[2] Prestress losses were calculated at midspan in stages as described in the specifications: losses immediately after transfer of prestress forces, losses from time of transfer to time of deck placement, and losses from the time of deck placement to 10,000 days (27 years), at which time 99% of losses have occurred. The gain in prestress force due to deck shrinkage was not considered for a couple of interrelated reasons. First, most if not all concrete decks experience cracking, which would relieve restrained stresses due to shrinkage. Second, the inclusion of stress gain due to the deck shrinkage will have little or no effect on the design of pretensioned, prestressed bridge girders because strength calculations are not affected and effects on concrete stress (serviceability) would be small. **Table 4** shows the results for the refined estimates of time-dependent prestress losses. This method produces stable creep losses from time of concrete slab placement throughout the life of the structure. The refined method does not account for the effects of mild reinforcing steel that could be included in the cross section.

Table 3. Approximate estimates of time-dependent prestress losses according to the 2014 *AASHTO LRFD Bridge Design Specifications*

Case	*ES*, ksi	*CR* + *SH* + *RE*, ksi	Losses at midspan, ksi
Base	20.2	25.6	45.8
T2	18.8	26.4	45.2
T4	17.8	27.3	45.1
MS 2.4	Prestress losses same as base case		
MS 5.0			

Note: *CR* = prestress loss due to creep; *ES* = prestress loss due to elastic shortening; *RE* = prestress loss due to relaxation; *SH* = prestress loss due to shrinkage. 1 ksi = 6.895 MPa.

Jayaseelan time-step method

In this method, time is divided into intervals that increase as the age of concrete increases. The prestress losses and the stresses in the concrete were calculated at the end of each time interval. The calculated stresses include the elastic stresses due to prestress, gravity loads, sustained loads, and relaxation of prestressing steel, along with the time-dependent effects due to creep and shrinkage of concrete. After the deck slab is placed, the entire composite section of concrete is treated as an elastic material. The elastic stresses and the stresses due to creep strain in concrete were individually calculated. This

Table 4. Refined estimates of time-dependent prestress losses at midspan calculated using gross-section properties according to the 2014 *AASHTO LRFD Bridge Design Specifications*

Case	Concrete age, days	*ES*, ksi	*CR*, ksi	*SH*, ksi	*RE*, ksi	Losses at midspan, ksi
Base	90	20.2	14.1	5.1	1.2	40.6
	10,000	20.2	13.3	7.1	2.4	43.1
T2	90	18.8	13.3	5.2	1.3	38.4
	10,000	18.8	12.5	7.2	2.5	41.0
T4	90	17.8	12.7	5.2	1.3	37.0
	10,000	17.8	12.0	7.2	2.6	39.6
MS 2.4	90	Prestress losses same as base case				
	10,000					
MS 5.0	90					
	10,000					

Note: *CR* = prestress loss due to creep; *ES* = prestress loss due to elastic shortening; *RE* = prestress loss due to relaxation; *SH* = prestress loss due to shrinkage. 1 ksi = 6.895 MPa.

method takes into account the varying material properties by recomputing the concrete properties each day. The initial age of the concrete at the transfer of prestress t_i was 1 day, the slab was placed at the concrete age t of 90 days, and superimposed loads were applied at t of 120 days. The final prestress losses were calculated at t of 10,000 days.

Time-dependent equations

The time-step method calculates the concrete compressive strength f'_c at an age of concrete t using ACI 209R Eq. (2-1):[14]

$$\left(f'_c\right)_t = \frac{t}{\alpha + \beta t}\left(f'_c\right)_{28} \qquad \text{(ACI 209R 2-1)}$$

where

α = 0.7 for Type III cement

β = 0.98 for steam cured

$(f'_c)_{28}$ = specified 28-day compressive strength of concrete

Time-dependent creep and shrinkage coefficients

The Jayaseelan time-step method used the following AASHTO LRFD specifications[2] time-dependent equations for the creep coefficient $\psi(t, t_i)$ and shrinkage strain ε_{sh} for the computation of prestress losses. The creep coefficient and shrinkage strain were calculated for each time interval as an increasing function of time. The initial age of concrete at the transfer of prestress t_i was taken as 1 day.

$$\psi(t, t_i) = 1.9 k_s k_{hc} k_f k_{td} t_i^{-0.118} \qquad \text{(AASHTO 5.4.2.3.2-1)}$$

where

$$k_s = 1.45 - 0.13(V/S) \geq 1.0 \qquad \text{(AASHTO 5.4.2.3.2-2)}$$

$$k_{hc} = 1.56 - 0.008H \qquad \text{(AASHTO 5.4.2.3.2-3)}$$

$$k_f = \frac{5}{1 + f'_{ci}} \qquad \text{(AASHTO 5.4.2.3.2-4)}$$

$$k_{td} = \frac{t}{61 + 4f'_{ci} + t} \qquad \text{(AASHTO 5.4.2.3.2-5)}$$

where

k_s = factor for the effect of the volume–to–surface area ratio V/S of the component

k_{hc} = humidity factor for creep

k_f = adjustment factor for concrete compressive strength

k_{td} = time development factor

H = relative humidity

f'_{ci} = specified concrete compressive strength at release

$$\varepsilon_{sh} = k_s k_{hs} k_f k_{td} 0.48 \times 10^{-3} \qquad \text{(AASHTO 5.4.2.3.3-1)}$$

where

$$k_{hs} = \text{humidity factor for shrinkage} = 2.00 - 0.014H \qquad \text{(AASHTO 5.4.2.3.3-2)}$$

Effective modulus or reduced modulus of elasticity

Gradual changes in stress during the service life of a structure produce additional creep strains. These additional strains are superimposed on the creep strains due to initial stresses and all previous stress changes. As the concrete ages, these additional strains are much smaller than those that would arise if the same stress changes occurred right after the instant of first loading. This effect is accounted for by the use of an age-adjusted effective modulus, which originated in ACI 209R-92.[14]

In this paper, the effective or reduced modulus of elasticity combines the effect due to elastic strain and creep of concrete as an elastic deformation on the concrete section. At constant loading, the elastic strain plus creep strain was calculated as $[1 + \psi(t, t_i)]$ times the elastic strain. The effective modulus of elasticity E_{eff} at time t for each day was calculated as follows:

$$E_{eff}(t) = \frac{E_c\left(t\right)}{\psi\left(t, t_i\right)}$$

where

$E_c(t)$ = modulus of elasticity of concrete at time t

The effective modulus of elasticity is reduced due to creep effects in the beam, and the transformed cross-section properties were calculated based on this reduced effective modulus of elasticity. The previous equation was used for the time-dependent analysis due to the effects of all the loads, including initial prestress, self-weight, concrete deck weight, and superimposed dead loads. The effective modular ratio n_{eff} was calculated using this reduced effective modulus of elasticity E_{eff} as follows:

$$n_{eff} = \frac{E_{ps}}{E_{eff}}$$

The effect due to time-dependent creep was included by using the modular ratio n_{eff} in the calculation of transformed cross-section properties.

Prestress loss equations

Prestress loss due to elastic shortening

The prestress loss due to elastic shortening ES was calculated as follows:

$$ES = \frac{E_{ps}}{E_{ct}} f_{cgp}$$

where

$$f_{cgp} = \left[P_{pi} - A_{ps}\left(SH + RE\right)\right] \times \left[\frac{1}{A_{tr}} + \frac{e_{tr}^2}{I_{tr}}\right] - \left[\frac{M_{SW} \times e_{tr}}{I_{tr}}\right] \quad (1)$$

where

E_{ct} = modulus of elasticity of concrete at transfer or time of load application

f_{cgp} = stress in concrete at the center of gravity of prestressing tendons due to the prestressing force immediately after transfer and the self-weight of the member at the section of maximum moment

A_{tr} = transformed cross-sectional area

e_{tr} = eccentricity of the prestressing strands calculated using transformed cross-section properties

I_{tr} = transformed moment of inertia of the section

M_{SW} = moment due to self-weight of the girder

In Eq. (1), the value for the prestressing force, $P_{pi} - A_{ps}$ ($SH + RE$) accounts for the reduction in prestressing force due to the effects of shrinkage of concrete and relaxation at a particular time t. The calculation of f_{cgp} for the loading stage after slab placement uses the composite transformed cross-section properties of concrete calculated using the effective modulus of elasticity.

Prestress loss due to creep

Incremental creep strains were computed daily using the following formula:

$$\Delta\varepsilon_{cr}\left(t\right) = \frac{1}{E_c\left(t\right)} f_{cgp}\left[\psi\left(t,1\right) - \psi\left(t-1,1\right)\right]$$

where

$\Delta\varepsilon_{cr}(t)$ = incremental creep strain at time t

The time-dependent creep loss $CR(t)$ was calculated as follows:

$$CR(t) = CR(t-1) + \Delta\varepsilon_{cr}(t)E_{ps}$$

The calculated final creep loss was calibrated to yield the same results as the creep loss calculated using the AASHTO LRFD specifications refined method. An ultimate creep coefficient factor of 2.61 as opposed to 1.9 was used to account for the variation in aggregate properties.

Prestress loss due to shrinkage

The shrinkage of concrete depends on the volume–to–surface area ratio *V*/*S* and relative humidity but is independent of the loading and primarily due to shrinkage of cement paste. The time-dependent shrinkage loss $SH(t)$ for each day was calculated with the following equation.

$$SH(t) = E_{ps}\varepsilon_{sh}(t)K_{sh}$$

where

$\varepsilon_{sh}(t)$ = shrinkage strain at time t calculated using the 2014 AASHTO LRFD specifications Eq. (5.4.2.3.3-1)[2]

$$K_{sht} = \frac{\left(\frac{1}{A_{tr}} + \frac{e_{tr}^2}{I_{tr}}\right)}{\left(\frac{1}{A_g} + \frac{e_g^2}{I_g}\right)}$$

where

K_{sht} = transformed cross-section coefficient that accounts for the time-dependent interaction between concrete and prestressing steel

A_g = gross cross-sectional area

e_g = eccentricity of the prestressing strands calculated using gross cross-section properties

I_g = gross moment of inertia of the section

Prestress loss due to relaxation of prestressing strands

Grade 270 (1860 MPa) low-relaxation strands are most widely used in prestressed concrete girders. The time-dependent relaxation loss $RE(t)$ is calculated by modifying the formula proposed in NCHRP report 496.[3]

$$RE\left(t\right) = \left[\frac{f_{pt}}{K_L'}\frac{\log\left(24t+1\right)}{\log\left(24t_i+1\right)}\left(\frac{f_{pt}}{f_{py}} - 0.55\right)\right]\left[1 - \frac{3\left(SH\left(t\right) + CR\left(t\right)\right)}{f_{pt}}\right]$$

where

f_{pt} = initial prestress in prestressing strands immediately after transfer

f_{py} = specified yield strength of prestressing steel

K'_L = factor accounting for type of prestressing steel used, 45 for low relaxation strands

The total prestress loss TL for the time-step method was calculated by summing up the individual components of prestress loss for each day.

$$TL = ES + CR(t) + SH(t) + RE(t)$$

The resulting prestress f_{se} and the corresponding prestressing force F_{se} were calculated for each day and each stage of loading.

Computation of concrete stresses and strains

The computations for the Jayaseelan time-step method were compiled and implemented in a spreadsheet routine. The equations and all of the relevant parameters were computed as a function of time. Calculations were made at each increment in time. Since the time variable t was taken in days, a new calculation for losses, strains, stresses, and for camber was made daily. For example, the top fiber stress f_t and bottom fiber stress f_b due to prestress, self-weight, and slab weight were calculated for each day. The corresponding strains ($\varepsilon_t = f_t/E_{eff}$, $\varepsilon_b = f_b/E_{eff}$) were calculated for the respective stresses. All calculations used the transformed cross-section properties of the girder section. The E_{eff} considers the effects of time on the modulus of concrete, so both *ES* and *CR* are included in this computation through $t = 0$ until slab casting. The composite transformed cross-section properties of concrete were used for the calculations after slab placement at 90 days. After slab placement, separate accounting was used to ensure proper application of elastic and time-dependent properties of both the slab and the girder. The additional strain due to creep was calculated by applying a resultant force on the composite cross section of the beam. This resultant force was calculated from the change in stress at time t due to creep in the beam. The final concrete strains at $t = 10{,}000$ days include the strain due to the prestressing force, gravity loads, slab weight, superimposed dead loads, and the additional strain due to time-dependent creep effects. Prestress losses and top and bottom stresses were computed daily for both girder ends and midspan of the section. **Table 5** shows the results for prestress losses

Table 5. Prestress losses at midspan calculated with the Jayaseelan time-step method

Case	Concrete age, days	*ES*, ksi	*CR*, ksi	*SH*, ksi	*RE*, ksi	Losses at midspan, ksi
Base	90	18.3	14.8	5.6	1.1	39.8
	10,000	18.3	13.3	7.8	2.2	41.6
T2	90	17.1	13.9	5.7	1.2	37.8
	10,000	17.1	12.2	7.8	2.4	39.5
T4	90	16.3	13.3	5.7	1.2	36.5
	10,000	16.3	11.5	7.9	2.4	38.2
MS 2.4	90	17.7	14.1	5.4	1.1	38.3
	10,000	17.7	12.6	7.5	2.3	40.1
MS 5.0	90	17.0	13.4	5.2	1.2	36.9
	10,000	17.0	12.0	7.2	2.4	38.7

Note: *CR* = prestress loss due to creep; *ES* = prestress loss due to elastic shortening; *RE* = prestress loss due to relaxation; *SH* = prestress loss due to shrinkage. 1 ksi = 6.895 MPa.

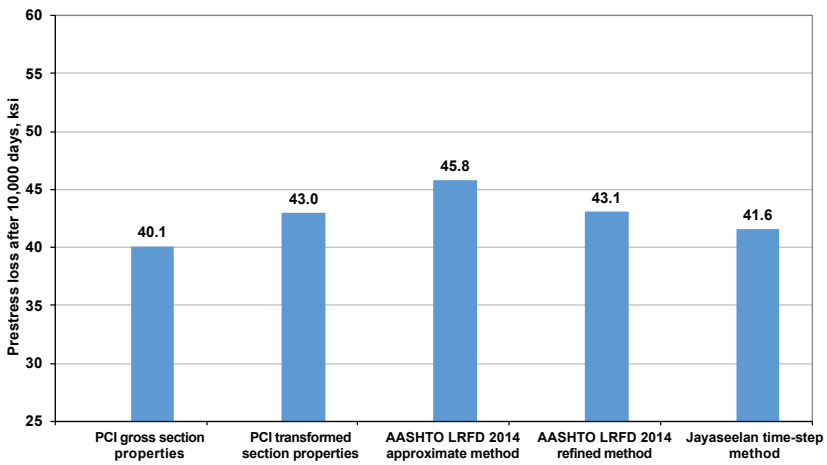

Figure 4. Comparison of total prestress losses at midspan for the base case. Note: 1 ksi = 6.895 MPa.

Table 6. Estimated camber at midspan calculated with the Jayaseelan time-step method

Case	Camber at 1 day (after release), in.	Camber at 90 days (before slab placement), in.	Camber at 91 days (after slab placement), in.	Long-term camber at midspan, in.
Base	-2.98	-4.08	-2.17	-1.81
T2	-2.73	-3.77	-1.81	-1.42
T4	-2.48	-3.44	-1.43	-1.00
MS 2.4	-2.88	-3.84	-1.98	-1.59
MS 5.0	-2.77	-3.58	-1.78	-1.37

Note: Negative values represent upward deflections. 1 in. = 25.4 mm.

computed using the Jayaseelan time-step method. **Figure 4** shows that the final prestress losses calculated using the Jayaseelan time-step method are comparable to the losses computed using the *PCI Design Handbook* and the 2014 AASHTO LRFD specifications methods.

Computation of girder cambers

Experience has shown that it is difficult to accurately predict cambers in prestressed concrete beams. This is principally due to the variation of the modulus of elasticity of concrete, creep of concrete, age of concrete, actual support conditions during storage, temperature and shrinkage differential between the top and bottom fibers, and variations in properties between the top and bottom of the concrete section.[18]

In the Jayaseelan time-step method, the camber of the beam was computed directly from curvatures that are computed from concrete strains in the cross section. Camber calculations were made with each time increment (daily), as were the strain computations. Camber calculations used the curvatures at the ends and the midspan. The effects of gravity are already embedded in the strain computations. Also, because we used the concrete strain computations as described, the variations in material properties over time were considered. After slab placement, the camber due to the additional creep strain was also included in the final deflection. **Table 6** reports the camber calculations at 1, 90, and 91 days and the long-term deflections at 10,000 days. **Figures 5** to **7** show the variation of camber with time for various cases. The figures show the downward deflection of the girder caused by the placement of the slabs and the self-weight of the deck concrete at 91 days. In addition, at 120 days, superimposed dead loads were applied so an additional downward deflection can be observed in all of the figures showing variation in camber over time.

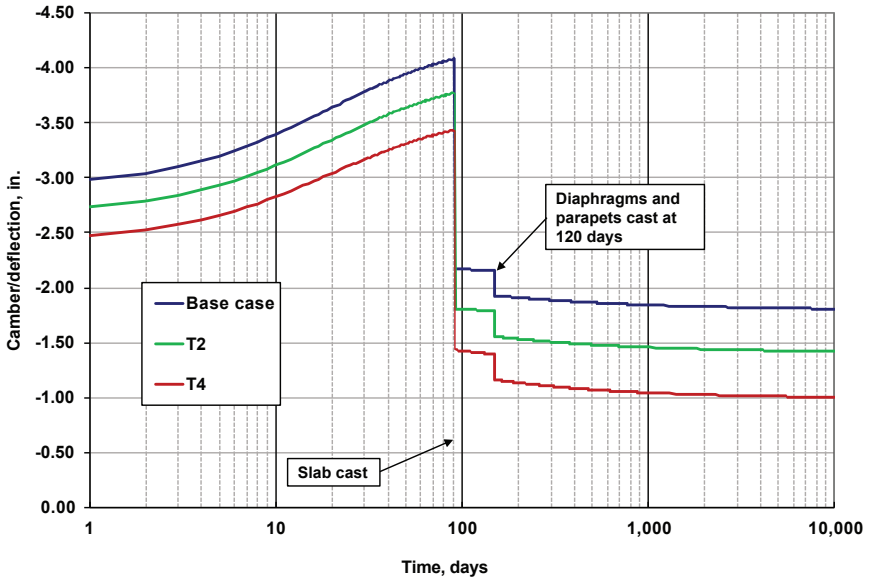

Figure 5. Effects of fully tensioned top strands on midspan deflection using the Jayaseelan time-step method. Note: 1 in. = 25.4 mm.

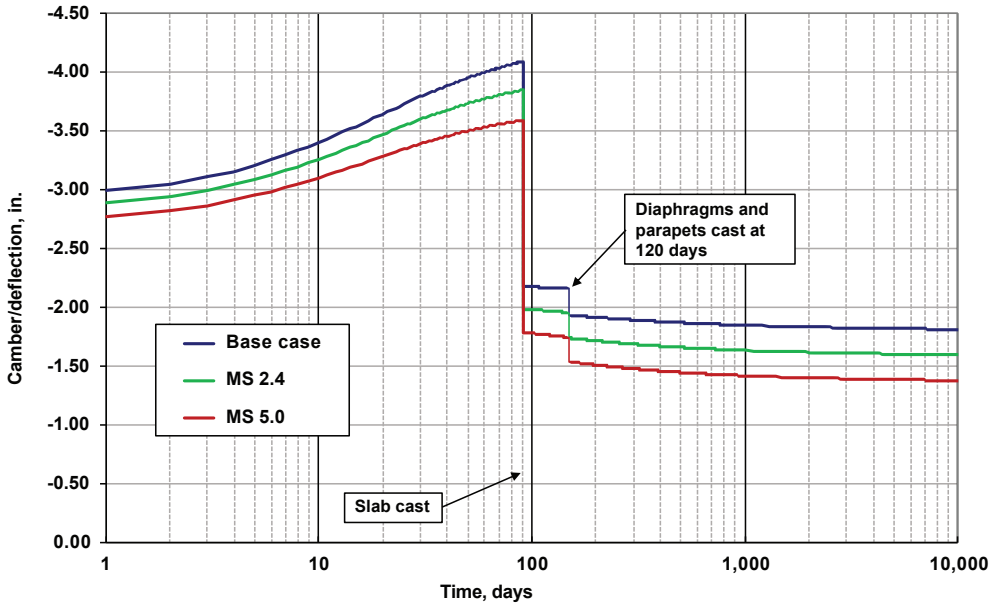

Figure 6. Effects of mild reinforcing steel on midspan deflection using the Jayaseelan time-step method. Note: 1 in. = 25.4 mm.

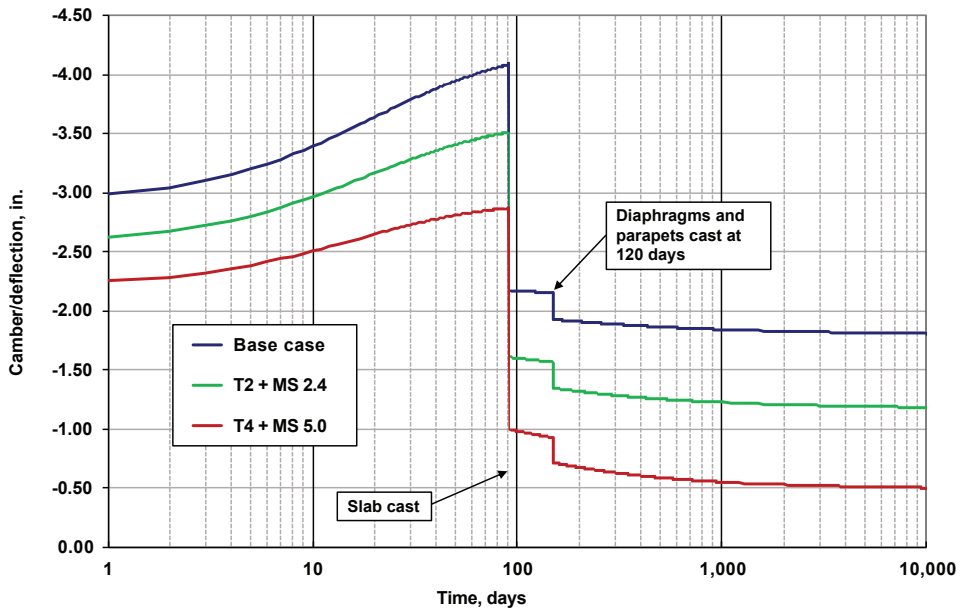

Figure 7. Effects of fully tensioned top strands and mild reinforcing steel on midspan deflection using the Jayaseelan time-step method. Note: 1 in. = 25.4 mm.

Results and discussion: Prestress losses

The five methods

Tables 1 to 5 present the prestress loss calculation results from the five different methodologies. The tables all report the prestress losses at midspan. Losses at the girder ends were computed but not reported. The methods include the *PCI Design Handbook* method based on the paper by Zia et al., the modified *PCI Design Handbook* method using transformed cross-section properties, both the 2014 AASHTO LRFD specifications approximate and refined methods, and the Jayaseelan time-step method developed by the authors. Where possible, the tables provide details of the various components of the prestress losses *ES*, *CR*, *SH*, and *RE*.

The results from the different methods are most remarkable for the similarities in the total prestress losses. For the base case design at 10,000 days, the total losses for each of the five

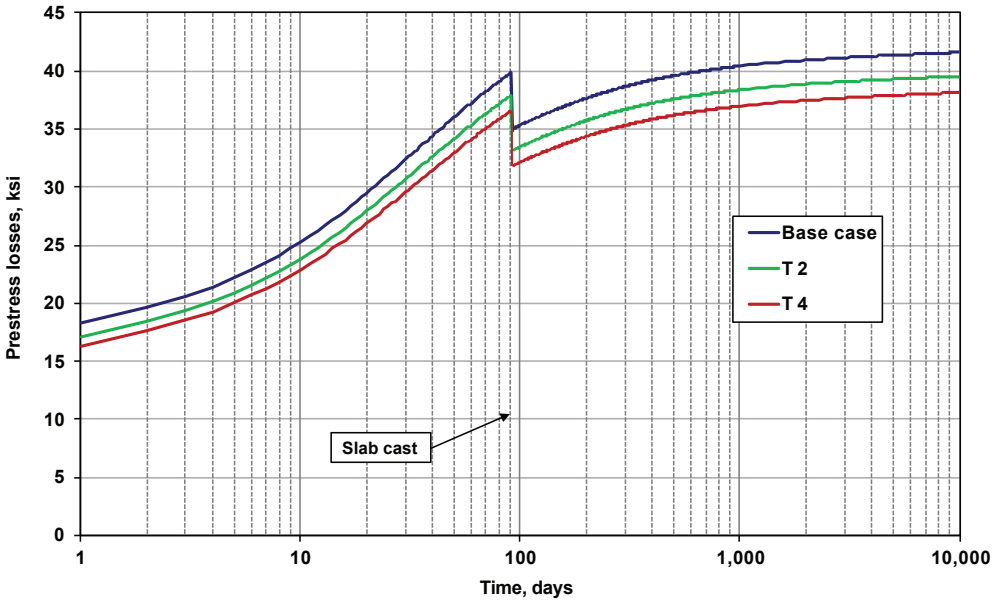

Figure 8. Prestress losses over time at midspan using the Jayaseelan time-step method. Note: Variations in losses are charted to show variations resulting from the inclusion of fully tensioned top strands. 1 ksi = 6.895 MPa.

methods fall between 40.1 and 45.8 ksi (276 and 316 MPa), or between 19.8% and 22.6% of the total prestress. Figure 4 presents the total losses for the base case at 10,000 days using the five different methods and shows their relative uniformity. At least for the base case design, the five methods produce very similar results for the estimated total losses. To understand the magnitude of the differences, it helps to consider the impact on the number of prestressing strands required to fulfill the design requirements. If the base case contains 34 bottom strands, a 2% difference in the total prestress losses reduces the number of strands required by about 0.7 strands. This variation means that a two-strand difference may occur in about one-third of similar design cases when using one of these five methods. This result is small enough to encourage a designer of precast, prestressed concrete bridge girders to use an approximate method for estimating prestress losses because a more precise analysis may only change one in three strand designs.

Effects of fully tensioned top strands

When fully tensioned top strands are added to the concrete section, the results show a clear trend indicating that the top strands reduce the total prestress losses. For the *PCI Design Handbook* method at 10,000 days, the T2 case reduces the total prestress losses from 40.1 to 38.7 ksi (276 to 267 MPa) and the T4 case further reduces them to 38.1 ksi (263 MPa). For the AASHTO refined method at 10,000 days, the inclusion of top strands reduces the base case from 43.1 to 41.0 ksi (297 to 283 MPa) with T2 and 39.6 ksi (273 MPa) with T4, so the use of four fully tensioned top strands (T4) reduces the prestress losses from 21.3% of total prestress to about 19.6% of total prestress. Therefore, including top strands provides a small but consistent reduction of the total prestress losses.

Adding fully tensioned top strands will also add tension to the bottom fiber of the pretensioned beam; however, the effects of additional tension are small. Note that if the fully tensioned top strands are located at the kern eccentricity, the result will be no additional tension. Strands are likely to be added above this eccentricity. Even so, the additional tension is small. In a similar bridge design for Type IV girders spanning approximately 103 ft (31 m), computations show that four fully tensioned top strands added about 130 psi (900 kPa) to the bottom fiber tension, and no changes to design were required.[19] The authors believe that the benefits of including fully tensioned top strands far outweigh any adverse effects from adding small amounts of tension to the bottom fiber. The use of fully tensioned top strands will be a decision made by individual designers or precast concrete producers, but it is clear from these results that the inclusion of fully tensioned top strands will mitigate excessive cambers, and those benefits may outweigh uncertainty and other costs.

This result is further supported by **Fig. 8**, which charts the prestress losses over time using the Jayaseelan time-step method. The total prestress losses are plotted against a log scale of time expressed in days. The figure shows that including fully tensioned top strands reduces the total losses compared with the base case and that this effect is carried through the life of the structure.

Effects of mild reinforcing steel

Based on engineering mechanics, mild reinforcing steel reduces prestress losses when included in prestressed concrete

sections. As the concrete section shortens, whether through elastic shortening, creep, or shrinkage, the shortening causes additional compressive strains and stresses in the composite anchored mild reinforcing steel, thus redistributing the forces within a prestressed concrete cross section that actively resists the prestressing forces. The mild reinforcing steel provides an ever increasing "transformed" cross section that reduces the time-dependent shortening of the concrete section and thereby reduces the total prestress losses.

Despite this, the calculations of three of the five methods for computing prestress losses are unaffected by the inclusion of mild reinforcing steel. These three methods—the *PCI Design Handbook* method (using gross-section properties), the AASHTO approximate method, and the AASHTO refined method—do not have a way to account for the inclusion of mild reinforcing steel, so if one of these methods is used, including mild reinforcing steel has no effect on the estimated total prestress losses.

The two remaining methods—the modified PCI method (using transformed cross-section properties) and the Jayaseelan time-step method—both incorporate the effects of mild reinforcing steel. The analysis shows a clear trend where the inclusion of mild reinforcing steel reduces prestress losses. For the modified *PCI Design Handbook* method at 10,000 days, the MS 2.4 case reduces the total losses from 43.0 to 41.9 ksi (296 to 289 MPa) and the MS 5.0 design further reduces the total losses to 40.8 ksi (281 MPa). For the Jayaseelan time-step method at 10,000 days, the inclusion of mild reinforcing steel reduces the base case from 41.6 to 40.1 ksi (287 to 276 MPa) with MS 2.4, and 38.7 ksi (267 MPa) with MS 5.0. So, the use of five no. 9 (29M) bars (MS 5.0) reduces prestress losses from 20.5% of total prestress to about 19.1% of total prestress. Therefore, including mild reinforcing steel produces small but consistent effects on total prestress losses.

This result is illustrated in **Fig. 9**, which charts the prestress losses over time with values computed using the Jayaseelan time-step method. The figure shows that the inclusion of mild reinforcing steel reduces total prestress losses and these reductions are carried through the life of the structure. Even so, the effects of including mild reinforcing steel only reduce the total prestress loss by about 2%.

Results and discussion: Bridge girder camber

The previous section shows that both the inclusion of fully tensioned top strands and mild reinforcing steel reduce the total prestress losses. A designer or bridge owner may not be convinced to use either option in their designs based solely on the small reduction in prestress losses. However, as this section will demonstrate, both top strands and mild reinforcing steel significantly influence the camber (or deflections) of prestressed concrete bridge girders. This may convince designers and bridge owners that using fully tensioned top strands and mild reinforcing steel in their designs will facilitate construction and increase the long-term serviceability of precast, prestressed concrete bridges.

In NCHRP report 496,[3] the primary recommendation for future research was to investigate camber in bridges. This section responds to that need and shows the rationale for adding fully tensioned top strands and mild reinforcing

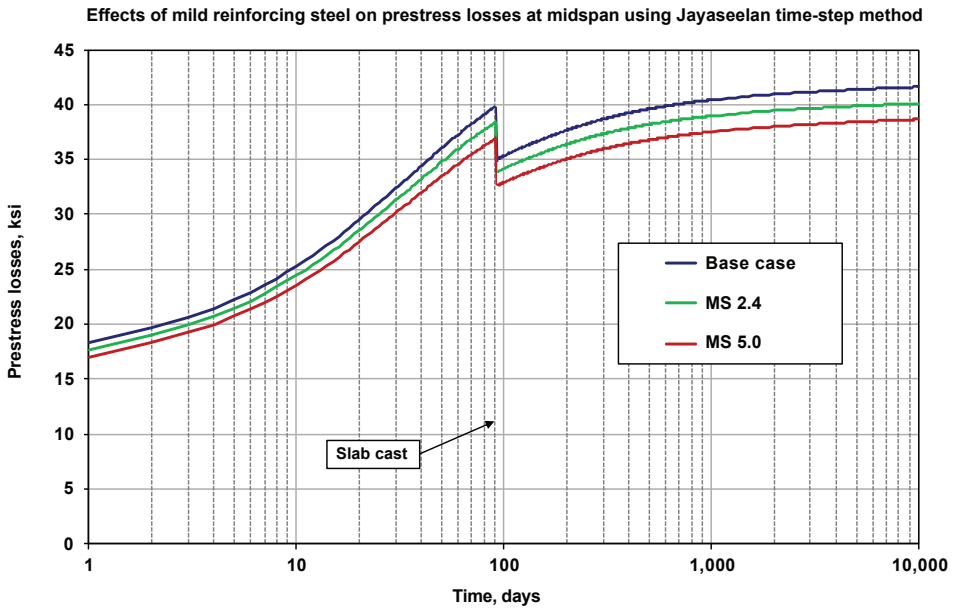

Figure 9. Effects of mild reinforcing steel on prestress losses at midspan using the Jayaseelan time-step method. Note: 1 ksi = 6.895 MPa.

steel to standard prestressed concrete bridge girder designs. The computations for stress and strain are embedded in the Jayaseelan time-step method presented in this paper. Table 5 reports prestress losses at midspan for this method, and using those calculations the curvature of the cross section at midspan can also be computed. To provide accurate estimates for girder camber, the prestress losses and material stresses were also required at the ends of the girders. The dead load deflections were also computed. The camber calculations reported in Table 6 and Fig. 5 to 7 account for varying prestress along the length of the bridge span and also include the downward deflections due to self-weight of the girder and all other superimposed dead loads.

Table 6 reports cambers at 1 day (immediately after release), at 90 days (before slab placement), at 91 days (after slab placement), and at 10,000 days, which is taken as the approximate life span of the bridge. Immediately after release, the camber for the base case was nearly 2.98 in. (76 mm). Through the effects of creep over the next 90 days, the camber increased more than 1 in. (25 mm) to 4.08 in. (104 mm) before the deck slab was placed. The analysis does not account for the probability that support conditions during handling, storage, and transport vary and also contribute to variations in camber of the prestressed girder. The analysis also assumes that the girders are supported at the ends. Table 6 also shows that the camber was 2.17 in. (55 mm) after slab placement (for the base case). This means that more than 2 in. (50 mm) of additional concrete haunch would exist at the ends of the girders compared with the midspan so that roadway elevations would be flat. During slab placement, the deflection resulting from the self-weight of the slab was 1.91 in. (49 mm) for the base case. The long-term camber at 10,000 days includes the effects of superimposed dead loads, principally the loads from diaphragms and parapets, which were applied at 120 days.

Figure 5 shows the effects of using fully tensioned top strands on midspan camber and deflections. As shown in Fig. 5 and Table 6, the inclusion of four top strands reduced initial camber (at one day) by about 0.50 in (13 mm). Figure 5 shows that as time increases, the differences in camber also increase, and at 90 days the camber in the base case was 4.08 in. (104 mm) and the camber in the T4 design was 3.44 in. (87 mm), a reduction of 0.64 in. (16 mm). As time increases, the differential that results from including top strands also increases so that the long-term reduction in camber was 0.81 in. (21 mm) out of a computed base case total of 1.81 in. (46 mm), representing a 45% reduction in the camber of the bridge.

Figure 6 shows the effects of including mild reinforcing steel on midspan camber and deflections. As shown in Fig. 6 and Table 6, the inclusion of five no. 9 (29M) bars (MS 5.0) reduced the initial camber (at one day) by about 0.20 in. (5 mm). Figure 6 shows that as time increases, the differences in camber also increase, and that at 90 days, the camber in the base case was 4.08 in. (104 mm) and the camber in the MS 5.0 design was 3.58 in. (91 mm), a reduction of 0.50 in. (13 mm). As time increases, the differences in camber resulting from the inclusion of mild reinforcing steel also increase. The long-term reduction in camber is significant. As Table 6 reports, the long-term camber of the base case was 1.81 in. (46 mm), and the MS 5.0 design resulted in long-term camber of only 1.37 in. (35 mm), a 0.44 in. (11 mm) reduction, which is about 25% less than the camber from the base case.

Figure 7 shows the effect on beam camber when fully tensioned top strands and mild reinforcing steel in the bottom flange are both included in the design. The initial cambers, immediately after release, are reduced from 2.98 in. (76 mm) for the base case to approximately 2.25 in. for T4 + MS 5.0 (57 mm), a reduction in initial cambers of about 0.75 in. (19 mm). At 90 days, the camber is reduced from 4.08 in. (104 mm) for the base case to less than 3.0 in. (76 mm) for T4 + MS 5.0, a reduction in camber of more than 1.0 in. (25 mm). In the long term, Fig. 7 shows that the reduction in camber approaches 1.5 in. (38 mm) by including top strands plus mild reinforcing steel. For the design under investigation, an AASHTO Type IV bridge girder with composite concrete deck slab spanning over 103 ft (31 m), the camber at the time of slab construction is reduced by more than 1.0 in. to less than 3.0 in. and the long-term camber is reduced to 0.50 in. (13 mm), which means that the long-term position of the Type IV girder is nearly flat.

Conclusion

- The inclusion of fully tensioned top strands decreased camber in the prestressed concrete girders. The design with four fully tensioned top strands (T4) reduced camber at 90 days (just before slab placement) from 4.08 in. (104 mm) for the base case to 3.44 in. (87 mm). The 0.64 in. (16 mm) reduction in camber represents 16% of the total camber for the base case before slab placement. The long-term camber was reduced from 1.81 to 1.00 in. (46 to 25 mm) for the base case and T4, respectively. This 0.81 in. (21 mm) reduction in camber represents 45% of the total camber for the base case. Therefore, using fully tensioned top strands reduces camber and provides greater assurance of long-term serviceability and ride quality.

- The inclusion of mild reinforcing steel at the center of gravity of the prestressing strands reduced camber in the prestressed concrete girders. The design with five no. 9 (29M) bars (MS 5.0) reduced camber at 90 days from 4.08 in. (104 mm) for the base case to 3.58 in. (91 mm). The 0.50 in. (13 mm) reduction in camber represents 12% of the total camber for the base case before slab placement. The long-term camber was further reduced from 1.81 in. (46 mm) for the base case to 1.37 in. (35 mm). This 0.44 in. (11 mm) reduction in camber represents 24% of the total camber for the base case. Therefore, using mild reinforcing steel within the cross section of the prestressed concrete girder reduces camber and provides greater assurance of long-term serviceability and ride quality.

- Combining the two preceding bullet points, the inclusion of both fully tensioned top strands with mild reinforcement (T4 + MS 5.0) reduced initial camber from 2.98 in. (76 mm) for the base case to approximately 2.3 in. (58 mm). Camber at 90 days was reduced from 4.08 in. (104 mm) for the base case to approximately 2.8 in. (71 mm). This 1.3 in. (33 mm) reduction in camber at the time of slab placement can simplify construction by decreasing the haunch depth required to compensate for camber differences along the length of the girder. Long-term camber was also reduced from 1.81 in. (46 mm) for the base case to approximately 0.50 in. (13 mm). This is an approximately 1.3 in. reduction in camber that represents 72% reduction in camber for the prestressed concrete bridge girder designed with fully tensioned top strands and mild reinforcing steel compared with the base case.

- The inclusion of fully tensioned top strands and mild reinforcing steel reduces short-term and long-term cambers, improving the constructibility of prestressed concrete bridges and providing greater assurance of their long-term serviceability and ride quality.

- The inclusion of fully tensioned top strands decreased prestress losses by marginal amounts. Using the AASHTO refined method, the total losses were reduced from 43.1 to 39.6 ksi (297 to 273 MPa) at 10,000 days for the base case and T4, respectively. Using the Jayaseelan time-step method, the total losses were reduced from 41.6 to 38.2 ksi (287 to 263 MPa) at 10,000 days for the base case and T4, respectively. The 3.4 to 3.5 ksi (23 to 24 MPa) reduction in total prestress losses represents about 8% reduction in prestress losses.

- The inclusion of mild reinforcing steel at the center of gravity of the prestressing strands reduced prestress losses by marginal amounts. Using the Jayaseelan time-step method, the total prestress losses were reduced from 41.6 to 38.7 ksi (287 to 267 MPa) at 10,000 days for the base case and MS 5.0, respectively. The 1.9 ksi (13 MPa) reduction represents about 5% reduction in prestress losses.

- Neither the AASHTO approximate method nor the AASHTO refined method can account for inclusion of mild reinforcing steel and its effects on prestress losses. For the design case examined, five different methods produced similar estimates of total prestress losses. For the base case, the *PCI Design Handbook* method, based on Zia et al., estimated total prestress losses of 40.1 ksi (276 MPa), 19.8% of total prestress, at 10,000 days, whereas the AASHTO refined method estimated total prestress losses of 43.1 ksi (297 MPa), 21.2%, at 10,000 days. The Jayaseelan time-step method estimated total prestress losses of 41.6 ksi (287 MPa), 20.5%, at 10,000 days.

- The AASHTO refined method requires modification to allow the prestress loss equations to account for the inclusion of mild reinforcing steel.

Acknowledgments

The authors gratefully acknowledge the sponsor of this research, the Oklahoma Department of Transportation.

References

1. Hassanain, M. A., R. E. Loov, D. Phil, and P. Eng. 1999. "Design of Prestressed Girder Bridges Using High Performance Concrete—An Optimization Approach." *PCI Journal* 44 (2): 40-55.

2. AASHTO (American Association of State Highway and Transportation Officials). 2014. *AASHTO LRFD Bridge Design Specifications*. 7th ed., customary U.S. units. Washington, DC: AASHTO.

3. Tadros, M. K., N. Al-Omaishi, S. Seguirant, and J. Gallt. 2003. *Prestress Losses in Pretensioned High-Strength Concrete Bridge Girders*. NCHRP (National Cooperative Highway Research Program) report 496. Washington, DC: Transportation Research Board.

4. Huo, X. S., N. Al-Omaishi, and M. K. Tadros. 2001. "Creep, Shrinkage, and Modulus of Elasticity of High-Performance Concrete." *Materials Journal* 98 (6): 440–449.

5. ACI-ASCE Joint Committee 423. 1958. "Tentative Recommendations for Prestressed Concrete." *Journal of the American Concrete Institute* 54: 545–1299.

6. PCI Committee on Prestress Losses. 1975. "Recommendations for Estimating Prestress Losses." *PCI Journal* 20 (4): 43–75.

7. AASHTO. 1977. *Standard Specifications for Highway Bridges*. 12th ed. Washington, DC: AASHTO.

8. Zia, P., H. K. Preston, N. L. Scott, and E. B. Workman. 1979. "Estimating Prestress Losses." *Concrete International* 1 (6): 32–38.

9. Shenoy, C. V., and G. C. Frantz. 1991. "Structural Tests of 27-Year-Old Prestressed Concrete Bridge Beams." *PCI Journal* 36 (5): 80–90.

10. Greuel, A., B. T. Rogers, R. A. Miller, B. M. Shahrooz, and T. M. Baseheart. 2000. "Evaluation of a High Performance Concrete Box Girder Bridge." *PCI Journal* 45 (6): 60–71.

11. Hale, W. M., and B. W. Russell. 2006. "Effect of Allowable Compressive Stress at Release on Prestress Losses and on the Performance of Precast, Prestressed Concrete Bridge Girders." *PCI Journal* 51 (2): 14–25.

12. Pessiki, S., M. Kaczinski, and H. H. Wescott. 1996. "Evaluation of Effective Prestress Force in 28-Year-Old Prestressed Concrete Bridge Beams." *PCI Journal* 41 (6): 78–89.

13. AASHTO. 1998. *AASHTO LRFD Bridge Design Specifications*. 2nd ed. Washington, DC: AASHTO.

14. ACI (American Concrete Institute) Committee 209. 1992. "Prediction of Creep, Shrinkage, and Temperature Effects in Concrete Structures." ACI 209R-92. Detroit, MI: ACI.

15. Tadros, M. K., A. Ghali, and W. H. Dilger. 1975. "Time-Dependent Prestress Loss and Deflection in Prestressed Concrete Members." *PCI Journal* 20 (3): 86–98.

16. Tadros, M. K., A. Ghali, and A. W. Meyer. 1985. "Prestressed Loss and Deflection of Precast Concrete Members." *PCI Journal* 30 (1): 114–141.

17. ACI Committee 318. 2014. *Building Code Requirements for Structural Concrete (ACI 318-14) and Commentary (ACI 318R-14)*. Farmington Hills, MI: ACI.

18. Lin, T. Y., and N. H. Burns. 1981. *Design of Prestressed Concrete Structures*. New York, NY: John Wiley & Sons.

19. Russell, Bruce W. 2018. "Using Fully Bonded Top Strands in Pretensioned Concrete Bridge Girders." *Aspire* 12 (3): 26–28.

Notation

A_g = gross cross-sectional area

A_{ps} = area of prestressing steel

A_{tr} = transformed cross-sectional area

CR = prestress loss due to creep of concrete

$CR(t)$ = prestress loss due to creep of concrete at time t

e = eccentricity of the prestressing strands

e_g = eccentricity of the prestressing strands calculated using gross cross-section properties

e_{tr} = eccentricity of the prestressing strands calculated using transformed cross-section properties

E_c = design modulus of elasticity of concrete

E_{ci} = initial modulus of elasticity of concrete

E_{ct} = modulus of elasticity of concrete at transfer or time of load application

$E_c(t)$ = modulus of elasticity of concrete at time t

E_{eff} = effective modulus of elasticity of concrete

$E_{eff}(t)$ = effective modulus of elasticity of concrete at time t

E_{ps} = modulus of elasticity of prestressing strands

ES = prestress loss due to elastic shortening

f_b = concrete stress at bottom fiber

f'_c = concrete compressive strength

$(f'_c)_{28}$ = specified 28-day compressive strength of concrete

f_{cds} = stress in concrete at center of gravity of prestressing tendons due to all superimposed permanent dead loads

f_{cgp} = stress in concrete at the center of gravity of prestressing tendons due to the prestressing force immediately after transfer and the self-weight of the member at the section of maximum moment

f'_{ci} = specified concrete compressive strength at release

f_{cir} = net compressive stress in concrete at center of gravity of prestressing tendons immediately after the prestress has been applied to the concrete

f_{cpi} = stress in concrete at center of gravity of prestressing tendons due to P_{pi}

f_g = stress in concrete at center of gravity of prestressing tendons due to weight of structure at time prestress is applied

f_{pt} = initial prestress in prestressing strands immediately after transfer

f_{pu} = ultimate strength of prestressing strand

f_{py} = specified yield strength of prestressing steel

f_{se} = effective stress in the prestressing strands after losses

f_t = concrete stress at the top fiber

F_{se} = effective prestressing force in the strands after losses

H = relative humidity

I_g = gross moment of inertia of the section

I_{tr} = transformed moment of inertia of the section

k_f = adjustment factor for concrete compressive strength

k_{hc} = humidity factor for creep

k_{hs} = humidity factor for shrinkage

k_s = factor for the effect of the volume–to–surface area ratio of the component

k_{td} = time development factor

K_{cir} = stress adjustment factor for elastic shortening and steel relaxation

K_{cr} = adjustment factor for creep

K_{es} = adjustment factor for elastic shortening

K'_L = factor accounting for type of prestressing steel used

K_{sh} = adjustment factor for shrinkage

K_{sht} = transformed cross-section coefficient that accounts for the time-dependent interaction between concrete and prestressing steel

M_{SW} = moment due to self-weight of the girder

n_{eff} = effective modular ratio

P_{pi} = prestressing force in tendons after seating loss but before reduction for *ES*, *CR*, *SH*, and *RE*

RE = prestress loss due to relaxation of prestressing strands

RE(*t*) = prestress loss due to relaxation of prestressing strands at time *t*

RH = relative humidity

SH = prestress loss due to shrinkage of concrete

SH(*t*) = prestress loss due to shrinkage of concrete at time *t*

t = age of the concrete in days

t_i = initial age of concrete at the transfer of prestress

TL = total prestress losses

V/*S* = volume–to–surface area ratio

w = unit weight of concrete

α = constant for the type of cement used from ACI 209R-92

β = constant for the type of curing method employed from ACI 209R-92

$\Delta\varepsilon_{cr}(t)$ = incremental creep strain at time *t*

ε_b = concrete strain at the bottom fiber

ε_{sh} = shrinkage strain

$\varepsilon_{sh}(t)$ = shrinkage strain at time *t*

ε_t = concrete strain at the top fiber

$\psi(t, t_i)$ = creep coefficient

About the authors

Hema Jayaseelan is a PhD candidate in the Civil and Environmental Engineering Department at Oklahoma State University in Stillwater. After completing her MS in Civil Engineering at Oklahoma State in 2007, she worked as a structural engineer in Kansas City, Mo., for one year and in Swansea, Wales, U.K., for a number of years.

Bruce W. Russell, PhD, PE, FACI, is an associate professor of civil and environmental engineering at Oklahoma State University. He has been a PCI member since 1990 and currently serves on the PCI Technical Activities Council, the PCI Bridges, Concrete Materials, and Fire Committees.

Abstract

This paper investigates the effects of fully tensioned top strands and inclusion of mild reinforcing steel on prestress losses and camber of pretensioned bridge girders. The results show that the inclusion of both fully tensioned top strands and mild reinforcing steel in the precompression zone reduced both short-term and long-term camber by 72% in the prestressed concrete bridge designs that were studied. Furthermore, the inclusion of both fully tensioned top strands and mild reinforcing steel have small but beneficial reduction in prestress losses. Prestress losses were estimated for a prestressed concrete bridge made with Type IV bridge girders spanning 103.33 ft (31.5 m). Five methods were used to estimate losses, including both the *AASHTO LRFD Bridge Design Specifications* approximate method and refined method. The newly developed Jayaseelan time-step method is presented and compared with other methods. The results show that all five methods estimate prestress losses that were within 2% of one another.

Keywords

Bridge, bridge girder, camber, concrete, deflection, girder, losses, prestressed.

Review policy

This paper was reviewed in accordance with the Precast/Prestressed Concrete Institute's peer-review process.

Reader comments

Please address any reader comments to *PCI Journal* editor-in-chief Emily Lorenz at elorenz@pci.org or Precast/Prestressed Concrete Institute, c/o *PCI Journal*, 200 W. Adams St., Suite 2100, Chicago, IL 60606.